The Fate of Glutamine in Human Metabolism. Comparison with Glucose.

Jean-Pierre Mazat[1,*] and Stéphane Ransac[1, *]

[1]IBGC CNRS UMR 5095 & Université de Bordeaux, 1, rue Camille Saint-Saëns 33077 BORDEAUX-cedex, France

* Correspondence: jean-pierre.mazat@u-bordeaux.fr; stephane.Ransac@u-bordeaux.fr ; Tel.: +33-556-999-041

Received: date; Accepted: date; Published: date

Abstract: Genome-scale models of metabolism (GEM) are now used to study how metabolism varies in different physiological conditions or environments. However, the great number of reactions involved in GEM makes it difficult to understand the results obtained in these studies. In order to have a more understandable tool, we develop a reduced metabolic model of central carbon metabolism, C2M2 with 63 reactions, 46 internal metabolites and 3 compartments, taking into account the actual stoichiometry of the reactions, including the stoichiometric role of the cofactors and the irreversibility of some reactions. In order to model OXPHOS functioning, the proton gradient through the inner mitochondrial membrane is represented by two pseudo-metabolites DPH (ΔpH) and DPSI (Δψ).

To illustrate the interest of such a reduced model of metabolism in mammalian cell, we used Flux Balance Analysis (FBA), to systematically study all the possible fates of glutamine in central carbon metabolism. Our analysis shows that glutamine can supply carbon sources for cell energy production and can be used as a carbon source to synthesize essential metabolites thus sustaining cell proliferation. We show how C2M2 can also be used to explore the results of more complex metabolic models in comparing our results with those of a medium size model MitoCore.

Keywords: Model of central carbon metabolism, Flux Balance Analysis, Glutamine.

1. Introduction

Genome-scale models of metabolism (GEM) greatly help to understand how metabolism varies in different physiological conditions, in different environments, in case of enzyme deficiencies and in interaction with other metabolisms. Used in conjunction with methods such as flux balance analysis [1], GEM are particularly useful to simulate metabolic changes in large metabolic networks as they do not require kinetic parameters and are computationally inexpensive. Many genome-scale constraint-based models [2–8] have covered central metabolism and have been used successfully to model diseases [9,10]. However, the great number of reactions involved in GEM makes it difficult to understand the results obtained in these kind of studies. In order to have a more manageable tool, we developed a reduced metabolic model of central carbon metabolism, C2M2, taking into account the true stoichiometry of the reactions, including the stoichiometric role of the cofactors and the irreversibility of some reactions. The configuration used in this work involves three compartments: the extracellular medium, the cytosol and the mitochondrial matrix. 63 reactions among 33 are irreversible and 46 internal metabolites are taken into account. Mitochondrial metabolism (OXPHOS) and mitochondrial transports, are often inaccurately represented in GEM with some exceptions [2,11]. In C2M2, the model of OXPHOS functioning is actually based on a proton gradient through the inner mitochondrial membrane, represented here by two pseudo-metabolites DPH (ΔpH) and DPSI (Δψ). This allows us to specifically take into account the 'vectorial' protons [12] across the mitochondrial membrane and not the protons in the reactions inside a given compartment which are, in principle, equilibrated.

To illustrate the interest of such a reduced model of metabolism in mammalian cell, we studied the metabolism of glutamine and compared it with the metabolism of glucose. Glutamine is the most abundant amino acid in plasma and has long been recognized to be essential in proliferating cell. Glutamine was identified as an alternative to glucose to fuel the Krebs cycle in cancer cells or in hypoxia conditions or mutations[13–19]. Glutamine metabolism goes through glutamate and α-ketoglutarate (AKG). Glutamate can be produced in the mitochondria by glutaminase or in the cytosol through nucleotide synthesis. When synthesized inside the mitochondria, glutamate may go out only through the H^+/Glutamate co-transporter [20] (the glutamate/aspartate exchanger with an H^+ entry is sensitive to the $\Delta\mu H^+$ and can be considered as irreversible in normal physiological conditions). Inside the mitochondria, glutamine-derived AKG replenish the TCA cycle and can be metabolized either through the canonical forward mode or via reductive carboxylation, leading to citrate and acetyl-CoA in the cytosol. For instance, Chen et al. [21] showed that glutamine enables mitochondrial DNA mutant cells survival thanks to both reductive and oxidative pathway in the TCA cycle.

Using Flux Balance Analysis (FBA), we systematically studied and discussed all the possible fates of glutamine in central carbon metabolism and we demonstrated that glutamine can supply carbon sources for cell energy production and be used as a carbon source to synthesize essential metabolites, thus sustaining cell proliferation. We show how C2M2 can also be used to explore the results of more complex metabolic models by comparing our results with those of MitoCore, a metabolic model of intermediate size built on the same bases.

2. Short description of the metabolic models

2.1. C2M2 Model

The reactions involved in the metabolic model C2M2 (Central Carbon Metabolic Model) are listed in Appendix B and depicted in Figure 1. The number of reactions is reduced by aggregation of successive reactions, while keeping the resulting stoichiometry, particularly of the involved cofactors. The abbreviations of the reaction names are listed in Appendix A. The model consists in a simple version of the Krebs cycle and connected reactions (reactions PDH, CS, IDH2 and 3, SLP, RC2, MDH2 and PYC with the addition of glutamate dehydrogenase (GLUD1)), in the glycolysis summarized in 5 steps, G1 (hexokinase + phosphoglucose isomerase), G2 (phosphofructokinase + aldolase + triose-phosphate isomerase), G3 (glyceraldehyde-3P dehydrogenase + phosphoglycerate kinase), ENOMUT (enolase + phosphoglycerate mutase) and PK (pyruvate kinase) extended by the reversible LDH (lactate dehydrogenase) and the possible output/input of lactate (LACIO). The gluconeogenesis consists in the reversible reactions of glycolysis plus PEPCK1 (phosphenolpyruvate carboxykinase), GG3 (triose phosphate isomerase + aldolase + fructose-1,6-biphosphatase) and GG4 (phosphogluco isomerase + glucose-6-phosphatase). The mitochondrial phosphenolpyruvate carboxykinase named PEPCK2 is included. The pentose phosphate pathway (PPP) reactions are summarized in PP1 (oxidative part of PPP) and PP2 (non-oxidative part of PPP).

The synthesis of nucleotide bases (NUC) is represented by a simplification of purine and pyrimidine biosynthesis obtained by averaging the stoichiometry of the different metabolites and cofactors in the metabolic pathway of each nucleotide and taking into account their different amounts in human (30% of A and T or U and 20% of G and C). It should be stressed that nucleotide synthesis necessitates glutamine which is converted to glutamate.

The synthesis of serine from 3-phosphoglycerate involves 3 steps: a dehydrogenase, a transaminase involving the glutamate/ α-ketoglutarate pair and a phosphatase. These three steps are assembled in one reaction: SERSYNT.

The malate/aspartate shuttle (MAS) is fully represented in the direction of NADHc consumption and NADHm production. It involves the malate/ α-ketoglutarate exchanger T2 (OGC) and the glutamate/aspartate exchanger T4 (AGC), the malate dehydrogenases (cytosolic MDH1 and mitochondrial MDH2) and the glutamate-oxaloacetate transaminases (cytosolic GOT1 and mitochondrial GOT2). A detailed representation of MAS was mandatory because MAS enzymes are

not always operating with the stoichiometry and the direction of MAS for exchange of NADHc for NADHm i.e. MAS components are not always used to run the MAS as such.

The synthesis of fatty acids is a major pathway in proliferating cells. It starts with citrate lyase (CL) and is represented in the case of palmitate by the reaction PL1 with the corresponding stoichiometries.

The respiratory chain is represented by three reactions, RC1 which is the respiratory complex I, RC2 (succinate dehydrogenase or complex II which also belongs to the TCA cycle + fumarase) and RC34 which represents complex III + IV.

Finally, the rest of oxidative phosphorylation are represented by ASYNT (ATP synthase), ANT, the ADP/ATP exchanger, T5 the Pi carrier and L the membrane leak of protons. The proton gradient is represented by two pseudo-metabolites DPH (ΔpH) and DPSI (Δψ). It allows us to only take into account the 'vectorial' protons across the mitochondrial membrane [12]. We introduced a possible ΔpH / Δψ exchange (NIG), mimicking the action of nigericin (K^+/H^+ exchanger) or physiologically, the action of ion exchangers in the inner mitochondrial membrane. DPH and DPSI are introduced, when necessary, in mitochondrial carriers equations. ATP hydrolysis is symbolized by ATPASE activity.

Only two entries are considered here, the entry of glutamine (GLNUP) and the entry of glucose (GLUCUP). The possible outputs in this study are pyruvate (T16), serine (SEROUT), aspartate (T14) nucleotides (T13) and palmitate (T17). The entry of glutamine in the mitochondria is through the transporter T8. It will give glutamate inside mitochondria through the operation of glutaminase GLS1.

2.2. MitoCore Model

MitoCore [11] is a manually curated constraint-based computer model of human metabolism that incorporates 324 metabolic reactions, 83 transport steps between mitochondrion and cytosol, and 74 metabolite inputs and outputs through the plasma membrane, to produce a model of manageable scale for an easier interpretation of results. The representation of the proton gradient is nearly the same as in C2M2 with the pseudo substrates PMF and DPH = 0.18 PMF and DPSI = 0.82 PMF. MitoCore's default parameters simulate normal cardiomyocyte metabolism with entry of different metabolites, particularly glucose and amino acids. These entries were lowered to zero and glutamine or glucose entry were set to one (unless otherwise mentioned) to compare the results of MitoCore with those of C2M2.

2.3. FBA analysis

We used FAME (Flux Analysis and Modeling Environment) (http://f-a-m-e.org/) [22] to derive the set of fluxes of C2M2 (and of MitoCore for comparison) optimizing the objective functions used below with glutamine or glucose entry. We systematically looked for the absolute flux minimization and then used the Flux Variability Analysis (FVA) to get an idea of the possible other solutions giving the same objective functions. Among these solutions (with a maximal objective function), we selected and drew the one with the maximal ATP synthesis rate. In the main text, we represented the solutions on a simplified version of Figure 1 (Figure 2 and the following). We gave the complete representations of the C2M2 fluxes in the supplementary materials with the corresponding figures labelled Figure Si for the simplified Figure i. Results are given in Table 1.

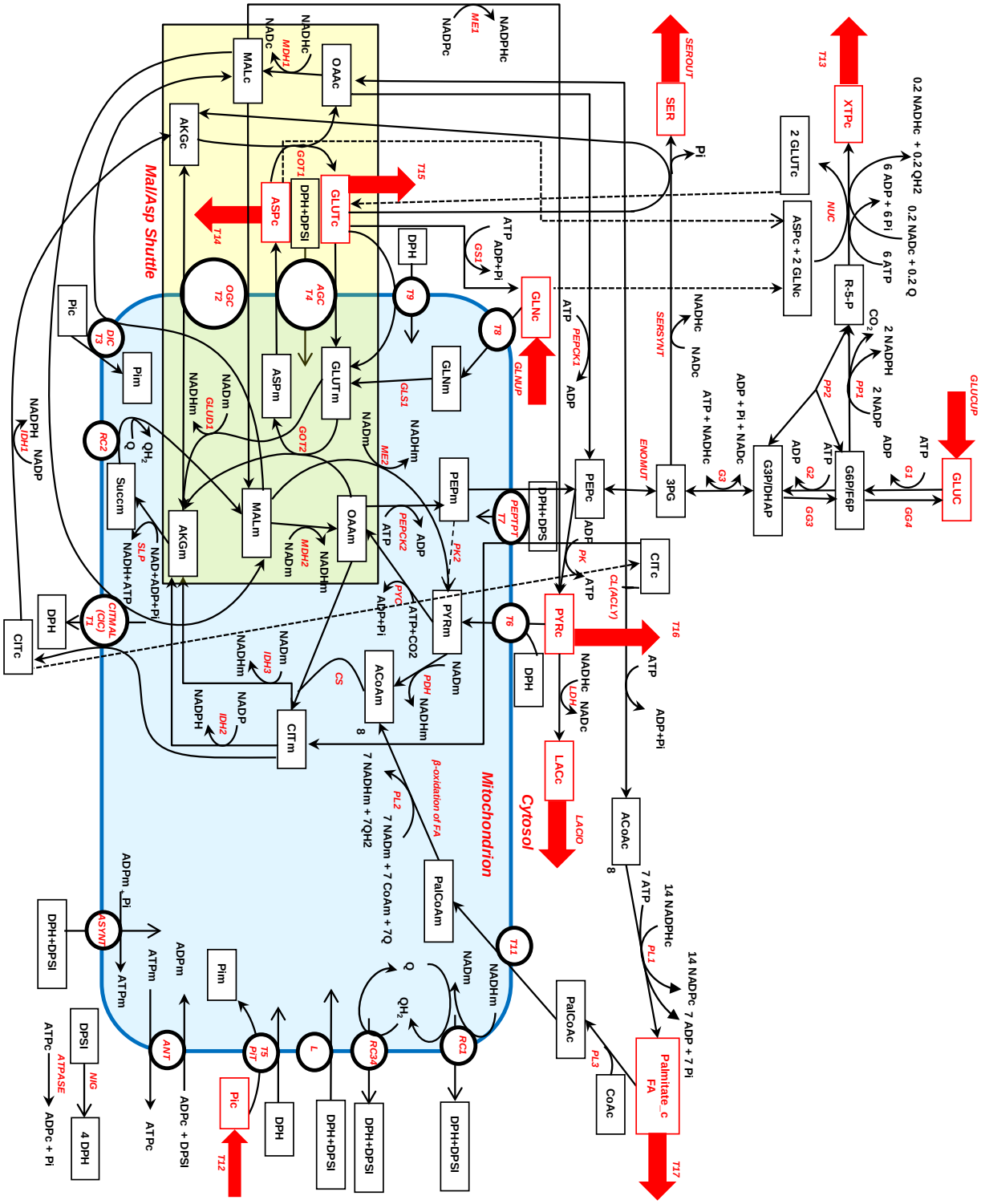

Figure 1. C2M2 Central Carbon Metabolic Model. Entry and output are indicated by red arrows. The corresponding metabolites are in red. The abbreviated name of the reactions are indicated in red italic along the arrows of the reaction. The mitochondrion is in blue and the malate/aspartate shuttle in light brown. Dotted lines link identical metabolites duplicated for the sake of presentation.

3. Results and discussions

3.1. Use of Glutamine for energy production (Figure 2).

Energy production is symbolized by ATPASE activity which is the objective function in this section. About 24 molecules of ATP can be synthesized from 1 molecule of glutamine without any other synthesis (Figure 2a and S2a). One molecule of glutamine enters the mitochondria and then the Krebs cycle as α-ketoglutarate (AKG) to double the flux to malate. One molecule of malate generates pyruvate (through ME2) and then acetyl-CoA which will condense with the OAA derived from the remaining molecule of malate to generate citrate and a canonical TCA cycle continue in the usual direction with a flux equal to 1. It is very similar to the TCA cycle fed with glycolysis-derived pyruvate except that, with glutamine, there is no need for NADHc reoxidation. In the same conditions, one molecule of glucose gives 33 ATP molecules at the most (Figure 2b and S2b). Nearly the same results are obtained with MitoCore: a TCA cycle with flux = 1 or 2 depending whether it comes from glutamine or glucose. It must be emphasized that in glutamine-derived ATP, the role of mitochondrial malic enzyme (ME2) is major for pyruvate and acetyl-CoA synthesis [23].

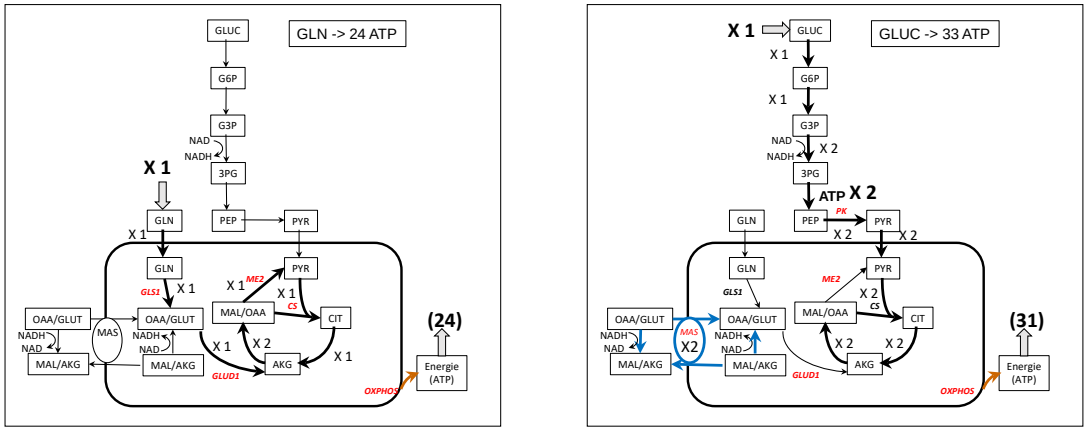

Figure 2. Simplified representation of ATP synthesis from glutamine (a) and glucose (b). Note that in (b), for the sake of simplicity, the representation of MAS has been separated from the TCA cycle although they share the MDH2 activity with a net flux of 4, 2 for MAS and 2 for the TCA cycle. See the complete figures of the fluxes in Figure S2.

3.2. Pyruvate synthesis from Glutamine (Figure 3).

The production of pyruvate (precursor of alanine) from glutamine can follow the production of glutamate and α-ketoglutarate (AKG) entering the "left", -oxidative- part of TCA cycle to produce OAA. From OAA, mitochondrial PEPCK2 produces PEP, which comes out of the mitochondria through citrate and malate cycling (grey arrows on Figure S3a) and generates pyruvate (with PK). One molecule of pyruvate is obtained per molecule of glutamine and 10.6 molecules of ATP can be synthesized in this condition. However, this solution requires to impose the maximum ATP synthesis flux. In the absence of this constraint, the emerging solution (with absolute fluxes minimization) is quite different (Figure S3c). Indeed, in this solution, pyruvate is synthesized through two pathways. The first one uses the reductive pathway of glutamine in the TCA cycle extruding 1.15 citrate of which 0.61 are cleaved by ATP citrate lyase (CL) to give OAAc that generates PEPc (PEPCK1) and then 0.61 pyruvate by PK and 0.077 palmitate. The second pathway uses the remaining 0.54 citrate to produce 0.54 pyruvate through cytosolic malic enzyme (ME1) amounting to 1.15 pyruvate. 0.15 pyruvate re-enter mitochondria. The second pathway through ME1 is necessary to produce the 1.08 NADPH (IDH1 and ME1) needed for palmitate synthesis. In this scenario, no ATP is synthesized and the reductive power of glutamine is consumed in citrate and palmitate synthesis. The mitochondrial

production of NADH is low as shown by the low activity of RC1 (0.084) as compared with 3.0 in the previous solution with high ATP synthesis flux.

Using MitoCore, we obtained a slightly different result with 1.41 pyruvate from glutamine and no ATP. In this solution, a great part of pyruvate is obtained with the successive syntheses of serine, glycine, alanine and then pyruvate. In this pathway, there is a high activity of monoamine oxidase specific of the central nervous system and a high activity of a mitochondrial lactate dehydrogenase which is rather unexpected in mammalian cells. Reducing monoamine oxidase activity to zero gives a similar solution as the initial solution of C2M2 with no ATP synthesis and a null activity of RCI. The maximal ATP synthesis flux is 10.9 when maintaining the maximal production of 1 pyruvate for 1 glutamine, which is comparable with the yields obtained with C2M2. The activity of the respiratory chain is also the same as in C2M2 (R_CI = 3, R_CII = 1 and R_CIII = 4, MitoCore notations). However with MitoCore, pyruvate is made through three different pathways. First with a low activity of the TCA cycle (0.101), then with mitochondrial malic enzyme (0.799) thanks to pyruvate released from mitochondria through an alanine cycle catalysed by the cytosolic and mitochondrial operation of ALATm and ALATc (alanine aminotransferase or glutamate-pyruvate aminotransferase) and finally with cytosolic malic enzyme (0.1).

With glucose as substrate (Figure 3b), the solution is rather simpler, with the synthesis of 2 glycolytic pyruvate and the reoxidation of NADHc by MAS and ETC accompanied by the corresponding ATP synthesis (6.9). The same solution is obtained with MitoCore when the maximal ATP synthesis is forced.

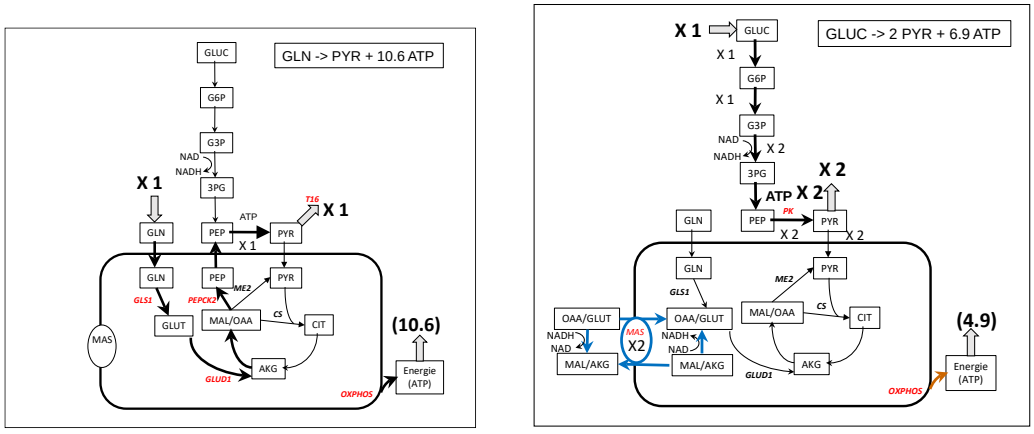

Figure 3. Simplified representation of pyruvate synthesis from glutamine (a) and glucose (b). Note that in (b), the glycolytic flux and the MAS flux are linked by NAD/NADH cycling. See the complete figures of the fluxes in Figure S3.

3.3 Apartate biosynthesis from glutamine (Figure 4).

Aspartate is an amino acid which participates in many reactions, particularly in nucleotides synthesis. Due to its low concentration in blood, aspartate synthesis is crucial for cell survival [24–26]. Aspartate synthesis from glutamine (Figure 4a and S4A) involves aspartate amino transferase (GOT) with oxalacetate (OAA) synthesized in the last part of TCA cycle from AKG coming from the glutamine-derived glutamate. Aspartate is carried out of the mitochondria through the glutamate-aspartate carrier (T4). Glutamate is recycled outside the mitochondria by the glutamate/H^+ carrier (T9). The maximal yield is one aspartate and 7.6 ATP per one glutamine.

Aspartate synthesis from glucose also requires the activity of GOTs (cytosolic or mitochondrial) but is more complicated. Several solutions can be considered. The maximal yield of aspartate is 1.86 per glucose (and 0 ATP) and is obtained with a paradoxical glutamine synthesis from glutamate with glutamine synthase (Figure S4c) which uses the 2 glycolytic ATP. Then the newly synthesized glutamine generates 1.86 aspartate as above with glutamine alone. When looking for a more direct

aspartate synthesis, without glutamine synthase (GS1 = 0) we obtained the solution represented in Figure 4b and in its full representation in Figure S4b. In this solution, 1.85 aspartate molecules and 2 glycolytic ATP are synthesized per glucose. In both solutions, reoxidation of glycolytic NADH imposes the operation of the malate-aspartate shuttle (MAS). NADH cannot be reoxidized by the lactate dehydrogenase because pyruvate carbons are necessary for aspartate synthesis. For this reason, in Figure 4b we have represented MAS with a flux equal to 2 and the glutamate-aspartate carrier (T4) with a supplementary activity of 1.85 to release 1.85 aspartate outside the mitochondria. More precisely on Figure S4b one can see that the flux of 2 pyruvate entering mitochondria is split in 1.85 pyruvate carboxylase flux which gives the 1.85 aspartate production through T4 and a 0.15 canonical TCA cycle (green arrows in Fig. 4b and S4b) generating the 1.85 ATPm necessary for the operation of 1.85 pyruvate carboxylase. MitoCore gives nearly the same yields (see table 1).

In recent papers [24–26] some authors evidenced "an essential role of the mitochondrial electron transport chain…. in aspartate synthesis". This is not unexpected if we note that mitochondrial synthesis of aspartate necessitates the synthesis of OAAm (using pyruvate carboxylase with ATP or malate dehydrogenase generating NADH) and the fact that the GLU/ASP exchanger (T4) depends on the $\Delta\mu H^+$, i.e. the ETC activity. We can confirm this result in our model as shown in Figure 4c in which we show the effect of decreasing the activity of RC34 on aspartate synthesis.

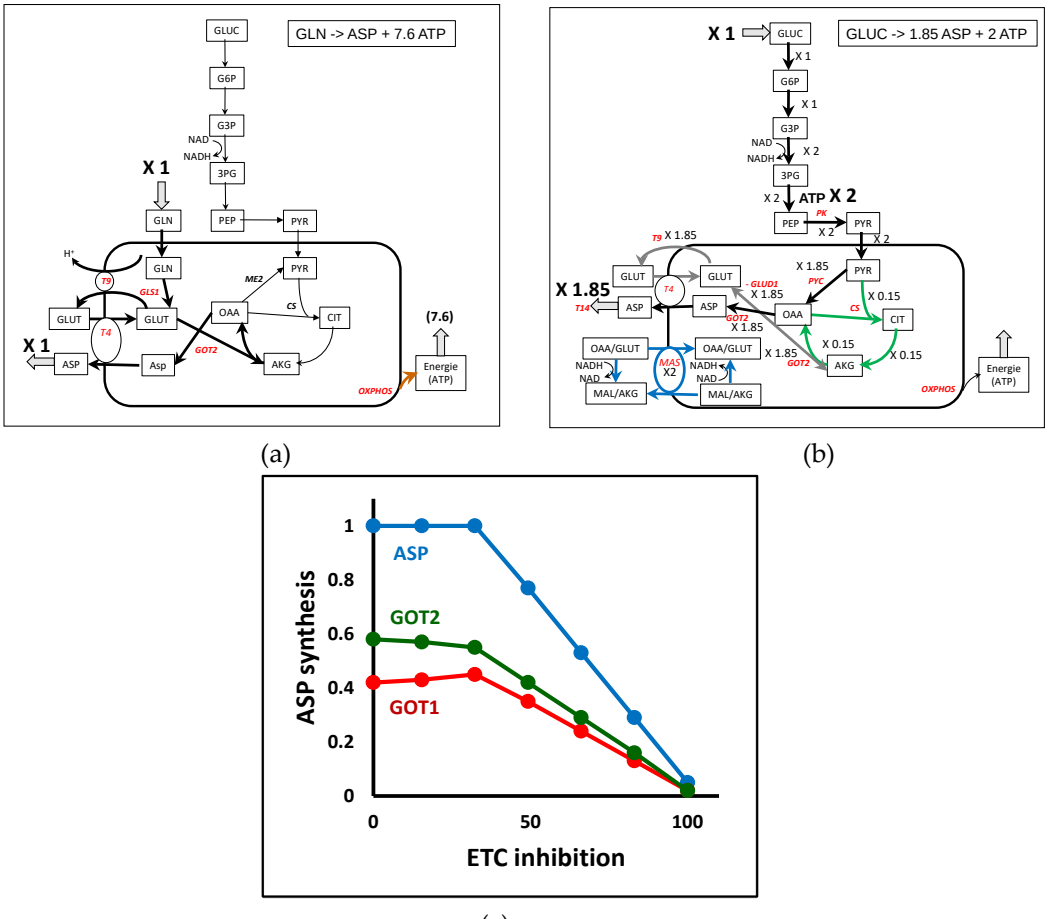

Figure 4. Simplified representation of aspartate synthesis from glutamine (a) and glucose (b). Note that in (b), the flux through T4 and GOT 2 can be split in a malate-aspartate shuttle (MAS) with a flux of 2 and in a 1.85 flux through T4 corresponding to aspartate output, i.e. T4 net flux is 3.85. See the complete representation of the glucose-derived aspartate in Figure S4b. **(c):** ETC inhibition of aspartate synthesis on glutamine (RC34 is inhibited). Note the interplay of GOT1 (cytosolic) and GOT2 (mitochondrial) activities to maintain a constant aspartate synthesis at the beginning of the curves.

3.4 Nucleotide synthesis from glutamine and glucose (Figure 5).

The synthesis of nucleotides requires glutamine, aspartate and R5P. In the absence of ASP and R5P, glutamine has to be used to ensure these syntheses. In the solution of figure 5a, 1/4 of glutamine is used for this purpose. The remaining 3/4 are used to synthesize 0.375 nucleotides (2 glutamine are necessary per nucleotide). 0.375 aspartate are regenerated with GOT1 using glutamate, leaving an equal amount of 0.375 glutamate entering the mitochondria. The oxalacetate formed in the TCA cycle enters the gluconeogenic pathway using PEPCK (inside the mitochondria or the cytosol) to form R5P.

The synthesis of nucleotides from glucose requires glutamine, aspartate and R5P synthesis. R5P is produced by the pentose phosphate pathway. Glutamine is recycled from glutamate by glutamine synthase (GS1) and aspartate is synthesized from oxalacetate produced by the anaplerotic activity of pyruvate carboxylase (PYC). There is the need to reoxidise glycolytic NADH and thus there is a flux (1.1) through the malate-aspartate shuttle (see Figures 5b and S5b) which reoxidizes glycolytic NADH and the NADHc produced by nucleotide synthesis. The yield of nucleotide synthesis with glucose is higher than with glutamine (0.63 XTP per glucose) but there is no ATP production.

The synthesis of nucleotides is not included in MitoCore so it is not possible to compare MitoCore with C2M2 in this respect. Note that nucleotide synthesis is a possible way to directly metabolise glutamine in the cytosol.

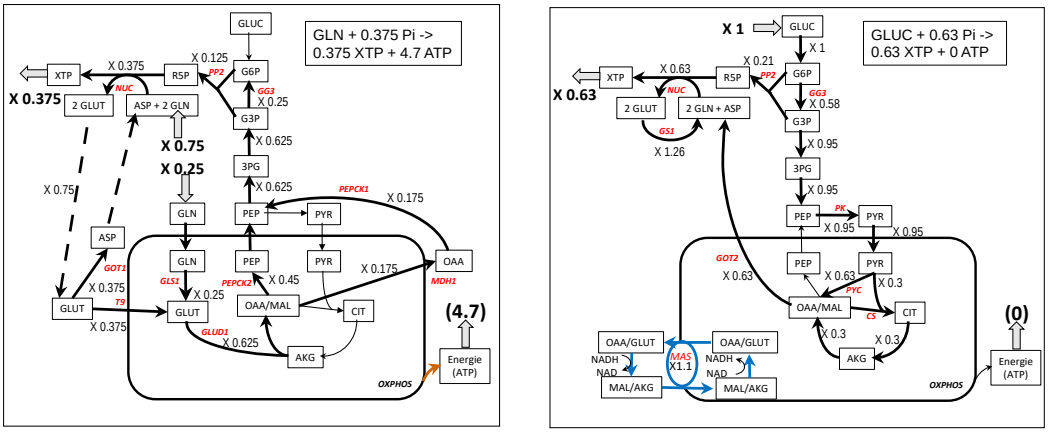

(a) (b)

Figure 5. Simplified representation of nucleotides synthesis from glutamine (a) and glucose (b). Note that in (b), the flux through T4 and GOT 2 can be split, in the malate-aspartate shuttle (MAS) with a flux of 1.1 and in a 0.63 flux through T4 corresponding to aspartate output. See the complete model in Figure S5 (a) and (b) in the supplementary materials.

3.5 Fatty acids synthesis from glutamine and glucose (Figure 6).

Fatty acids (FA) synthesis is an important pathway in proliferating cells, especially for phospholipids syntheses. For example, for palmitate synthesis, 0.17 palmitate molecule can be synthesized from one molecule of glutamine and because this is rather energy consuming, no ATP molecule is synthesized (Figure 6a). The synthesis occurs through ATP citrate lyase (CL) fed by citrate synthesized in TCA cycle. The glutamine-derived AKG flux in the TCA cycle (flux = 1) is split between the reductive pathway giving directly citrate by inversion of IDH3 (flux = - 0.4) and the oxidative pathway through malate and oxalacetate (flux = 0.6) and pyruvate coming from the recycling of OAAc product of CL in the cytosol. Involvement of reductive use of glutamine and participation of IDH1 in fatty acids synthesis is well documented [13,14,27] in hypoxia and mutations in TCA cycle or in respiratory chain [28] and appears to be linked to the AKG/citrate ratio [29]. The TCA cycle can be viewed as converging to citrate synthesis by the two pathways from AKG. This dual TCA pathway used for citrate synthesis has been well documented by Corbet & Feron [30,31]. It is interesting to see that in our model, the canonical TCA cycle is fuelled by the pyruvate derived from the OAA produced by citrate splitting into OAA and Acetyl-CoA. The NADPH needed for palmitate synthesis is synthesized by IDH1 in cytosol. It could have been made by the malic enzyme (ME1) or by the

oxidative pentose phosphate pathway (PP1) in cytosol but this occurs with a slightly lower yield (0.16). The involvement of malic enzyme (ME1) in NADPH synthesis is also well documented. In [32] the authors showed that 60% of NADPH is synthesized from glutamine by malic enzyme and that the pyruvate produced is excreted as lactate. We do not observe a release of lactate in our models because in the absence of glucose there is no excess of carbon and pyruvate enters the mitochondria to replenish the TCA cycle in the classical anaplerotic way. The authors also observed a G6PDH flux (PP1) of the same order as the glutaminolysis flux, demonstrating that several sources of NADPH can be active *in vivo*.

With glucose as carbon substrate (Figure 6b), oxalacetate coming from ATP-acetate lyase (CL) generates malate thanks to the cytosolic malate dehydrogenase (MDH1), oxidizing the glycolytic NADH as found in [28,33]. The cytosolic malate re-enters mitochondria through antiporters, particularly in exchange with citrate. It is an elegant way to absorb the cytosolic reductive power of glucose avoiding the operation of MAS. These pathways are often observed when NADH reoxidation is impeded (respiratory complex deficiency for instance). This has also been observed in patients (lipid droplets) with mitochondrial diseases.

MitoCore gives identical yields in palmitate (called hexadecanoic acid in MitoCore) synthesis (see table 1).

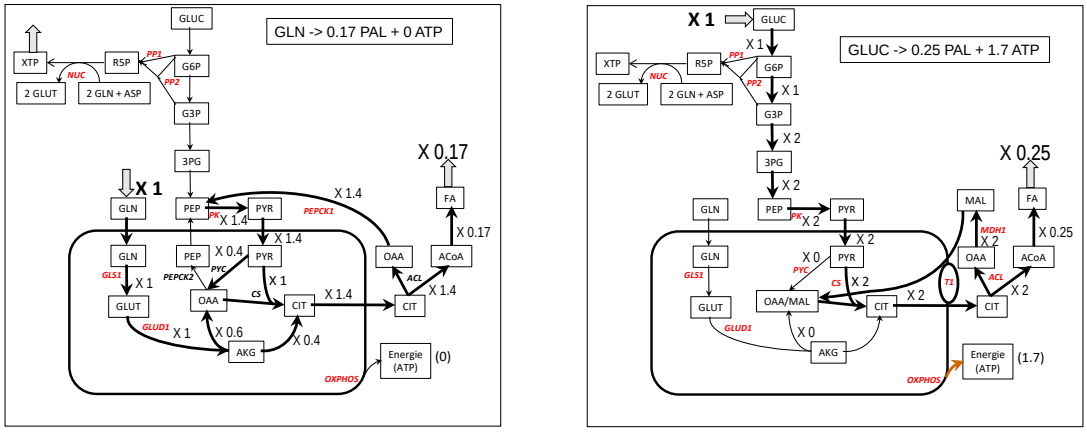

Figure 6. Simplified representation of palmitate synthesis from glutamine (a) and glucose (b). See the complete model in Figure S6a and b in the supplementary materials.

3.6 Serine synthesis from glutamine and glucose (Figure 7).

Serine is the major source of one-carbon units for methylation reactions via tetrahydrofolate and homocysteine. It is the precursor of glycine (see [34] for a mini-review). In his pioneer work, Snell demonstrated the importance of serine biosynthesis in rat carcinoma [35]. More recently several authors emphasized the role of serine in breast cancers and in melanoma cells and emphasized the role of PEPCK [3,12,36–38]. It is easy to demonstrate, using C2M2, that decreasing PEPCK activity (in either the cytosol or the mitochondrion) proportionally decreases serine synthesis.

We have already studied the different yield in serine synthesis on different substrates with our core model [39]. The synthesis of serine from glutamine is represented in Figure 7a. It involves the synthesis of PEP as in pyruvate synthesis, but here PEP is used to make 3PG, a serine precursor. The glutamate used in the transamination reaction is recycled from the AKG produced and the NADH produced by the dehydrogenase reaction is reoxidized with MDH1. In addition, 9.3 ATP can be synthesized. With glucose as a carbon substrate, 3PG is synthesized directly from glucose via glycolysis (Figure 7b). However the work of Hanson in rats demonstrates that "pyruvate entry into the gluconeogeneic pathway is the major route for serine biosynthesis" [34,40]. It is difficult to obtain this pathway from glucose in C2M2. This could indicate that in the case of this work, serine is mainly

synthesized form other sources than glucose (glutamine or other amino acids for instance). The yield of serine synthesis with glucose as a carbon substrate can reach 2 molecules of serine per one molecule of glucose with 4.4 ATP molecules in addition. 4 NADHc are generated which necessitate a flux of 4 in the MAS (Figure 7b).

MitoCore gives similar results (see table 1).

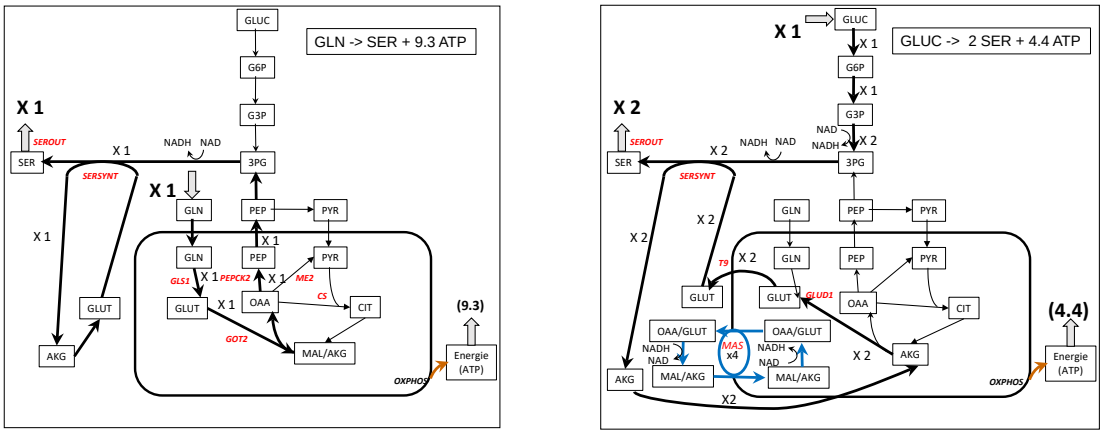

(a) (b)

Figure 7. Simplified representation of serine synthesis from glutamine (a) and glucose (b). See the complete model in Figure S6 in the supplementary materials.

Table 1. Maximal yield in metabolites synthesis or energy (ATP) from glutamine and glucose at steady-state. The first value is obtained with C2M2 and the second with MitoCore.

Objective Function	1 x GLN		1 x GLUC	
	Metabolite	ATP	Metabolite	ATP
ATPASE	0 / 0	23.8 / 24.0	0 / 0	33.34 / 33.04
Pyruvate (T16)	1 / 1	10.6 / 10.9	2 / 2	6.9 / 6.85
Aspartate (T14)	1 / 1	7.6 / 7.7	1.85 / 1.82	2 / 2
XTP (T13)	0.375	4.7	0.64	0
Palmitate (T17)	0.17 / 0.17	0 / 0	0.25 / 0.24	0 / 0
Serine (SEROUT)	1 / 1	9.3 / 9.1	2 / 2	4.4 / 3.8

4. Conclusion

We developed a core metabolic model of central carbon metabolism, C2M2, with a limited number of reactions (63) and of metabolites (46 internal metabolites) to explore the potential of glutamine to supplant glucose in metabolic syntheses and energy production. A salient feature of this model is that it takes into account the actual stoichiometries of the reactions particularly the stoichiometries of cofactors, even for concatenated reactions. A second characteristic of this model is that it uses a relevant model of oxidative phosphorylation taking into account the mitochondrial $\Delta\mu H^+$ in the form of pseudo substrates DPH and DPSI as was already done in MitoCore [11] and in [2]. This allowed us to properly model cell energy production and to take into account the constraints introduced by the necessary regeneration of cofactors.

The advantage of C2M2 is that, due to the low number of reactions and metabolites, the interpretation of the results are rather straightforward and can be easily represented and understood on a metabolic scheme. All the solutions maximizing an objective function (described by FVA) can be more easily explored as was done here in the case of pyruvate and aspartate synthesis. Furthermore quantitative balance of any internal metabolites can be performed as in the case of glutamine-derived pyruvate and glucose-derived aspartate synthesis (Figures S3 and S4). Such a

balance makes it possible to identify the metabolic pathways at work for the synthesis of a given metabolite. They are often represented in our figures with different colors. The drawback of C2M2 is that not all solutions of a metabolic question will be obtained: the complexity of cell metabolism cannot be represented by a very simple model. However a simple model such as C2M2 can help exploring and understand the huge amount of solutions offered by greater models, especially genome –scale models. We compared C2M2 with MitoCore, a middle-size metabolic model with 407 reactions and transports and 452 metabolites. In the case of glutamine-derived pyruvate we showed how C2M2 helps recognize the solutions which also exist in MitoCore and those that do not exist in C2M2.

With C2M2, we demonstrated that glutamine is a precursor as good as glucose for the syntheses of the main metabolites necessary for cell proliferation and energy production and we are able to give the quantitative yield in these productions (table 1). The same yields are obtained with MitoCore that constitutes a cross validation of both models. Taking into account cofactors makes it possible to emphasize the role of the malate/aspartate shuttle (MAS) in glucose metabolism by making it a controlling (limiting) step in the use of glucose for metabolic syntheses and energy production, reorienting when necessary glycolysis towards lactate production (Crabtree or/and Warburg effect). This was also well exemplified by the "gas pedal" mechanism where Ca^{2+} activates glutamate/aspartate carrier (T4) enhancing pyruvate formation and mitochondrial respiration [41]. More generally our study emphasizes the role of mitochondrial transporters and the role of some metabolites cycling to output other metabolite, for instance, glutamate cycling to remove mitochondrial aspartate or malate cycling to remove mitochondrial citrate.

C2M2 cannot replace more complex models, particularly genome-scale models, in the exploration of the huge number of metabolic possibilities offered by a metabolic network. Nevertheless, it can constitute a first step to analyze experimental results as experimentalists use to do in metabolic sketches but with the quantitative constraints eliminating some impossible solutions. It can also be a first step in analyzing the solutions of genome scale metabolic models by the recognition of common solutions and the reasons of non-common ones. Passing through a middle size metabolic model such as MitoCore can be an additional option corresponding each time to an increase by an order of magnitude in the number of reactions (63 reactions for C2M2, 407 for MitoCore and around 7 440 for Recon 2 [4]).

We would like to stress, however, that a big advantage of C2M2 is that it can be approached by several other theoretical methods than FBA, especially by deterministic ones i.e. the writing of the differential equations of metabolic concentrations as a function of the rate functions and the calculation of control coefficients. The elementary flux modes (EFMs), although numerous, (some millions in the case of C2M2) can also be performed. The interest of several approaches is they shed various light on metabolic solutions and furthermore necessitate an agreement between the different metabolic explanations.

To sum it up, even if C2M2 has several limitations in its solutions, it offers a significant alternative to using genome scale models in facilitating quantitative studies of metabolic networks and in obtaining a consensus between several theoretical approaches.

Supplementary Materials:

Figure S1: C2M2 metabolic network.

Figure S2: complete C2M2 metabolic network of energy production from glutamine and glucose.

Figure S3: complete C2M2 metabolic network of pyruvate synthesis from glutamine and glucose.

Figure S4: complete C2M2 metabolic network of aspartate synthesis from glutamine and glucose.

Figure S5: complete C2M2 metabolic network of nucleotides synthesis from glutamine and glucose.

Figure S6: complete C2M2 metabolic network of Fatty Acids synthesis from glutamine and glucose.

Figure S7: complete C2M2 metabolic network of serine synthesis from glutamine and glucose.

SBML code S1: C2M2_GLN.xml

SBML code S2: C2M2_GLUC.xml

SBML code S3: MitoCore_GLN.xml

SBML code S4: MitoCore_GLUC.xml

Author Contributions: JPM and SR equally contributed to this work.

Funding: This work was supported by the Plan cancer 2014–2019 No BIO 2014 06 and the French Association against Myopathies.

Acknowledgments: We would like to thank several colleagues for helpful discussions on our model: Bertrand Beauvoit, Sophie Colombié, Martine Dieuaide-Noubhani, Yves Gibon, Christine Nazaret, Pierre Petriacq, Sylvain Prigent and Michel Rigoulet. Thanks to Anne Devin for discussions and English corrections.

Conflicts of Interest: The authors declare no conflict of interest.

Appendix A: Abbreviations

AGC: aspartate-glutamate carrier (see **T4** in appendix B)
AKG: α-ketoglutarate or 2-oxoglutarate
ANT: ADP/ATP exchanger.
ASYNT: ATP Synthase.
ASPUP: Uptake of aspartate.
ATPASE: ATP usage.
CL (ACL): (ATP) Citrate Lyase.
CS: Citrate Synthase.
DPH: pH difference between inside and outside mitochondria.
DPSI: mitochondrial membrane potential.
ENOMUT: Enolase + Phosphoglycerate Mutase.
ETC: Electron Transport Chain or Respiratory Chain
FBA: Flux Balance Analysis.
FVA: Flux Variability Analysis.
G1: hexokinase + phosphoglucose isomerase.
G2: phosphofructokinase + aldolase + triose-phosphate isomerase.
G3: Glyceraldehyde-3P Dehydrogenase + phosphoglycerate kinase.
GG3: triose phosphate isomerase + aldolase + fructose -1,6-biphosphatase.
GG4: phosphogluco isomerase + glucose-6-phosphatase.
GLS1: Glutaminase.
GLNUP: Uptake of Glutamine.
GLUCUP: Uptake of glucose.
GLUD1: Glutamate Dehydrogenase.
GOT: Glutamate Oxaloacetate Transaminase.
IDH: Aconitase + Isocitrate dehydrogenase.
L: Proton leak of the mitochondrial membrane.
LACIO: Input/Output of lactate.
LDH: Lactate Dehydrogenase**.**
MAS: Malate/Aspartate Shuttle.

ME: Malic Enzyme.
MDH: Malate Dehydrogenase
NIG: for nigericine, exchange of DPH and DPSI.
NUC: Nucleotide (XTP) Synthesis.
OGC: Oxoglutarate carrier (see **T2** in appendix B).
PDH: Pyruvate Dehydrogenase.
PEPCK: PhosphoEnolPyruvate Carboxy Kinase.
PK: Pyruvate Kinase.
PL1: Synthesis of PhosphoLipids.
PP1: Oxidative part of PPP.
PP2: non-oxidative part of PPP.
PPP: Pentose Phosphate Pathway.
PYC: Pyruvate Carboxylase.
RC1: Complex I of Respiratory Chain.
RC2: succinate dehydrogenase + fumarase.
RC34: Complex III+IV of Respiratory Chain.
SEROUT: Output of serine.
SERSYNT: Serine Synthesis= Dehydrogenase + Transaminase and Phosphatase.
SLP: 2-oxoglutarate dehydrogenase + succinate thiokinase

Appendix B: METATOOL ENTRY FILE OF C2M2

```
-ENZREV
   ANT ASYNT ENOMUT G3 GLUD1 GOT1 GOT2 IDH1 IDH2 IDH3 LACIO LDH MDH1 MDH2
   NIG PP2 RC1 RC2 T1 T2 T3 T5 T7 T8 T9 T12 T14 T15 T16 T17

-ENZIRREV
   ASPUP ATPASE CL CS G1 G2 GG3 GG4 GLNUP GLS1 GLUCUP GS1 L ME1 ME2 NUC PDH
   PEPCK1 PEPCK2 PK PL1 PL2 PL3 PP1 PYC RC34 SEROUT SERSYNT SLP T4 T6 T11 T13

-METINT
   3PG ACoAc ACoAm ADPc ADPm AKGc AKGm ASPc ASPm ATPc ATPm CITc CITm DPH DPSI
   G3P G6P GLNc GLNm GLUCc GLUTc GLUTm LACc MALc MALm NADc NADHc NADm
   NADHm NADPc NADPm NADPHc NADPHm OAAc OAAm Palmitate_c PEPc PEPm Pic Pim
   PYRc PYRm R5P SERc SUCCm XTPc

-METEXT
   ASP CO2 CoAc CoAm GLN GLUC GLUT HCO3 LAC NH3 O PalCoAc PalCoAm Palmitate Pi
   PYR Q QH2 SER XTP

-CAT
ANT : ATPm + ADPc + DPSI = ATPc + ADPm .
ASPUP : ASP = ASPc .
ASYNT : 3 ADPm + 3 Pim + 8 DPH + 8 DPSI = 3 ATPm .
ATPASE : ATPc = ADPc + Pic .
CL : CITc + ATPc + CoAc = ACoAc + OAAc + ADPc + Pic .
CS : ACoAm + OAAm = CITm .
ENOMUT : PEPc = 3PG .
G1 : GLUCc + ATPc = G6P + ADPc .
G2 : G6P + ATPc = 2 G3P + ADPc .
G3 : G3P + NADc + ADPc + Pic = 3PG + NADHc + ATPc .
```

GG3 : 2 G3P = G6P + Pic .
GG4 : G6P = GLUCc + Pic .
GLNUP : GLN = GLNc .
GLS1 : GLNm = GLUTm + NH3 .
GLUCUP : GLUC = GLUCc .
GLUD1 : GLUTm + NADm = AKGm + NADHm + NH3 .
GOT1 : GLUTc + OAAc = ASPc + AKGc .
GOT2 : GLUTm + OAAm = ASPm + AKGm .
GS1 : GLUTc + NH3 + ATPc = GLNc + ADPc + Pic .
IDH1 : CITc + NADPc = AKGc + NADPHc + CO2 .
IDH2 : CITm + NADPm = AKGm + NADPHm + CO2 .
IDH3 : CITm + NADm = AKGm + NADHm + CO2 .
L : DPSI + DPH = .
LACIO : LACc = LAC .
LDH : PYRc + NADHc = LACc + NADc .
MDH1 : MALc + NADc = OAAc + NADHc .
MDH2 : MALm + NADm = OAAm + NADHm .
ME1 : MALc + NADPc = PYRc + NADPHc + CO2 .
ME2 : MALm + NADm = PYRm + NADHm + CO2 .
NIG : DPSI = 4 DPH .
NUC : R5P + 2 GLNc + ASPc + 6 ATPc + 0.2 NADc + 0.2 Q = XTPc + 2 GLUTc + 6 ADPc + 6 Pic + 0.2 NADHc + 0.2 QH2 .
PDH : PYRm + NADm = ACoAm + NADHm + CO2 .
PEPCK1 : OAAc + ATPc = PEPc + ADPc + CO2 .
PEPCK2 : OAAm + ATPm = PEPm + ADPm + CO2 .
PK : PEPc + ADPc = PYRc + ATPc .
PL1 : 8 ACoAc + 7 ATPc + 14 NADPHc + 7 HCO3 = Palmitate_c + 7 ADPc + 7 Pic + 14 NADPc + 8 CoAc + 7 CO2 .
PL2 : PalCoAm + 7 NADm + 7 CoAm + 7 Q = 7 NADHm + 8 ACoAm + 7 QH2 .
PL3 : Palmitate_c + CoAc = PalCoAc .
PP1 : G6P + 2 NADPc = R5P + 2 NADPHc + CO2 .
PP2 : 3 R5P = 2 G6P + G3P .
PYC : PYRm + HCO3 + ATPm = OAAm + Pim + ADPm .
RC1 : NADHm + Q = NADm + QH2 + 4 DPH + 4 DPSI .
RC2 : SUCCm + Q = MALm + QH2.
RC34 : QH2 + O = Q + 6 DPH + 6 DPSI .
SEROUT : SERc = SER .
SERSYNT : 3PG + GLUTc + NADc = SERc + AKGc + NADHc + Pic .
SLP : AKGm + NADm + Pim + ADPm = SUCCm + NADHm 1+CO2 + ATPm
T1 : CITm + MALc = CITc + MALm + DPH .
T2 : AKGc + MALm = AKGm + MALc .
T3 : MALm + Pic = MALc + Pim .
T4 : GLUTc + ASPm + DPH + DPSI = GLUTm + ASPc .
T5 : Pic + DPH = Pim .
T6 : PYRc + DPH = PYRm .
T7 : PEPc + Pim = PEPm + Pic .
T8 : GLNc = GLNm .
T9 : GLUTc + DPH = GLUTm .
T11 : PalCoAc = PalCoAm .
T12 : Pi = Pic .
T13 : XTPc = XTP .
T14 : ASPc = ASP .

T15 : GLUTc = GLUT .
T16 : PYRc = PYR .
T17 : Palmitate_c = Palmitate .

References

1. Orth, J.D.; Thiele, I.; Palsson, B.Ø. What is flux balance analysis? *Nat. Biotechnol.* **2010**, *28*, 245–248, doi:10.1038/nbt.1614.
2. Swainston, N.; Smallbone, K.; Hefzi, H.; Dobson, P.D.; Brewer, J.; Hanscho, M.; Zielinski, D.C.; Ang, K.S.; Gardiner, N.J.; Gutierrez, J.M.; et al. Recon 2.2: from reconstruction to model of human metabolism. *Metabolomics Off. J. Metabolomic Soc.* **2016**, *12*, 109, doi:10.1007/s11306-016-1051-4.
3. Duarte, N.C.; Becker, S.A.; Jamshidi, N.; Thiele, I.; Mo, M.L.; Vo, T.D.; Srivas, R.; Palsson, B.Ø. Global reconstruction of the human metabolic network based on genomic and bibliomic data. *Proc. Natl. Acad. Sci. U. S. A.* **2007**, *104*, 1777–1782, doi:10.1073/pnas.0610772104.
4. Thiele, I.; Swainston, N.; Fleming, R.M.T.; Hoppe, A.; Sahoo, S.; Aurich, M.K.; Haraldsdottir, H.; Mo, M.L.; Rolfsson, O.; Stobbe, M.D.; et al. A community-driven global reconstruction of human metabolism. *Nat. Biotechnol.* **2013**, *31*, 419–425, doi:10.1038/nbt.2488.
5. Ma, H.; Sorokin, A.; Mazein, A.; Selkov, A.; Selkov, E.; Demin, O.; Goryanin, I. The Edinburgh human metabolic network reconstruction and its functional analysis. *Mol. Syst. Biol.* **2007**, *3*, 135, doi:10.1038/msb4100177.
6. Mardinoglu, A.; Agren, R.; Kampf, C.; Asplund, A.; Nookaew, I.; Jacobson, P.; Walley, A.J.; Froguel, P.; Carlsson, L.M.; Uhlen, M.; et al. Integration of clinical data with a genome-scale metabolic model of the human adipocyte. *Mol. Syst. Biol.* **2013**, *9*, 649, doi:10.1038/msb.2013.5.
7. Mardinoglu, A.; Agren, R.; Kampf, C.; Asplund, A.; Uhlen, M.; Nielsen, J. Genome-scale metabolic modelling of hepatocytes reveals serine deficiency in patients with non-alcoholic fatty liver disease. *Nat. Commun.* **2014**, *5*, 3083, doi:10.1038/ncomms4083.
8. Uhlén, M.; Fagerberg, L.; Hallström, B.M.; Lindskog, C.; Oksvold, P.; Mardinoglu, A.; Sivertsson, Å.; Kampf, C.; Sjöstedt, E.; Asplund, A.; et al. Proteomics. Tissue-based map of the human proteome. *Science* **2015**, *347*, 1260419, doi:10.1126/science.1260419.
9. Yizhak, K.; Chaneton, B.; Gottlieb, E.; Ruppin, E. Modeling cancer metabolism on a genome scale. *Mol. Syst. Biol.* **2015**, *11*, 817, doi:10.15252/msb.20145307.
10. Bordbar, A.; Monk, J.M.; King, Z.A.; Palsson, B.O. Constraint-based models predict metabolic and associated cellular functions. *Nat. Rev. Genet.* **2014**, *15*, 107–120, doi:10.1038/nrg3643.
11. Smith, A.C.; Eyassu, F.; Mazat, J.-P.; Robinson, A.J. MitoCore: a curated constraint-based model for simulating human central metabolism. *BMC Syst. Biol.* **2017**, *11*, 114, doi:10.1186/s12918-017-0500-7.
12. Mitchell, P. Coupling of phosphorylation to electron and hydrogen transfer by a chemi-osmotic type of mechanism. *Nature* **1961**, *191*, 144–148.
13. Metallo, C.M.; Gameiro, P.A.; Bell, E.L.; Mattaini, K.R.; Yang, J.; Hiller, K.; Jewell, C.M.; Johnson, Z.R.; Irvine, D.J.; Guarente, L.; et al. Reductive glutamine metabolism by IDH1 mediates lipogenesis under hypoxia. *Nature* **2011**, *481*, 380–384, doi:10.1038/nature10602.
14. Mullen, A.R.; Wheaton, W.W.; Jin, E.S.; Chen, P.-H.; Sullivan, L.B.; Cheng, T.; Yang, Y.; Linehan, W.M.; Chandel, N.S.; DeBerardinis, R.J. Reductive carboxylation supports growth in tumour cells with defective mitochondria. *Nature* **2011**, *481*, 385–388, doi:10.1038/nature10642.

15. Cluntun, A.A.; Lukey, M.J.; Cerione, R.A.; Locasale, J.W. Glutamine Metabolism in Cancer: Understanding the Heterogeneity. *Trends Cancer* **2017**, *3*, 169–180, doi:10.1016/j.trecan.2017.01.005.
16. Eagle, H. The specific amino acid requirements of a human carcinoma cell (Stain HeLa) in tissue culture. *J. Exp. Med.* **1955**, *102*, 37–48.
17. Kvamme, E.; Svenneby, G. Effect of anaerobiosis and addition of keto acids on glutamine utilization by Ehrlich ascites-tumor cells. *Biochim. Biophys. Acta* **1960**, *42*, 187–188.
18. Daye, D.; Wellen, K.E. Metabolic reprogramming in cancer: unraveling the role of glutamine in tumorigenesis. *Semin. Cell Dev. Biol.* **2012**, *23*, 362–369, doi:10.1016/j.semcdb.2012.02.002.
19. Altman, B.J.; Stine, Z.E.; Dang, C.V. From Krebs to clinic: glutamine metabolism to cancer therapy. *Nat. Rev. Cancer* **2016**, *16*, 773, doi:10.1038/nrc.2016.131.
20. Fiermonte, G.; Palmieri, L.; Todisco, S.; Agrimi, G.; Palmieri, F.; Walker, J.E. Identification of the mitochondrial glutamate transporter. Bacterial expression, reconstitution, functional characterization, and tissue distribution of two human isoforms. *J. Biol. Chem.* **2002**, *277*, 19289–19294, doi:10.1074/jbc.M201572200.
21. Chen, Q.; Kirk, K.; Shurubor, Y.I.; Zhao, D.; Arreguin, A.J.; Shahi, I.; Valsecchi, F.; Primiano, G.; Calder, E.L.; Carelli, V.; et al. Rewiring of Glutamine Metabolism Is a Bioenergetic Adaptation of Human Cells with Mitochondrial DNA Mutations. *Cell Metab.* **2018**, *27*, 1007-1025.e5, doi:10.1016/j.cmet.2018.03.002.
22. Boele, J.; Olivier, B.G.; Teusink, B. FAME, the Flux Analysis and Modeling Environment. *BMC Syst. Biol.* **2012**, *6*, 8, doi:10.1186/1752-0509-6-8.
23. Yang, C.; Ko, B.; Hensley, C.T.; Jiang, L.; Wasti, A.T.; Kim, J.; Sudderth, J.; Calvaruso, M.A.; Lumata, L.; Mitsche, M.; et al. Glutamine oxidation maintains the TCA cycle and cell survival during impaired mitochondrial pyruvate transport. *Mol. Cell* **2014**, *56*, 414–424, doi:10.1016/j.molcel.2014.09.025.
24. Birsoy, K.; Wang, T.; Chen, W.W.; Freinkman, E.; Abu-Remaileh, M.; Sabatini, D.M. An Essential Role of the Mitochondrial Electron Transport Chain in Cell Proliferation Is to Enable Aspartate Synthesis. *Cell* **2015**, *162*, 540–551, doi:10.1016/j.cell.2015.07.016.
25. Van Vranken, J.G.; Rutter, J. You Down With ETC? Yeah, You Know D! *Cell* **2015**, *162*, 471–473, doi:10.1016/j.cell.2015.07.027.
26. Sullivan, L.B.; Gui, D.Y.; Hosios, A.M.; Bush, L.N.; Freinkman, E.; Vander Heiden, M.G. Supporting Aspartate Biosynthesis Is an Essential Function of Respiration in Proliferating Cells. *Cell* **2015**, *162*, 552–563, doi:10.1016/j.cell.2015.07.017.
27. Wise, D.R.; Ward, P.S.; Shay, J.E.S.; Cross, J.R.; Gruber, J.J.; Sachdeva, U.M.; Platt, J.M.; DeMatteo, R.G.; Simon, M.C.; Thompson, C.B. Hypoxia promotes isocitrate dehydrogenase-dependent carboxylation of α-ketoglutarate to citrate to support cell growth and viability. *Proc. Natl. Acad. Sci. U. S. A.* **2011**, *108*, 19611–19616, doi:10.1073/pnas.1117773108.
28. Gaude, E.; Schmidt, C.; Gammage, P.A.; Dugourd, A.; Blacker, T.; Chew, S.P.; Saez-Rodriguez, J.; O'Neill, J.S.; Szabadkai, G.; Minczuk, M.; et al. NADH Shuttling Couples Cytosolic Reductive Carboxylation of Glutamine with Glycolysis in Cells with Mitochondrial Dysfunction. *Mol. Cell* **2018**, *69*, 581-593.e7, doi:10.1016/j.molcel.2018.01.034.
29. Fendt, S.-M.; Bell, E.L.; Keibler, M.A.; Olenchock, B.A.; Mayers, J.R.; Wasylenko, T.M.; Vokes, N.I.; Guarente, L.; Vander Heiden, M.G.; Stephanopoulos, G. Reductive glutamine metabolism is a function of the α-ketoglutarate to citrate ratio in cells. *Nat. Commun.* **2013**, *4*, 2236, doi:10.1038/ncomms3236.

30. Corbet, C.; Draoui, N.; Polet, F.; Pinto, A.; Drozak, X.; Riant, O.; Feron, O. The SIRT1/HIF2α axis drives reductive glutamine metabolism under chronic acidosis and alters tumor response to therapy. *Cancer Res.* **2014**, *74*, 5507–5519, doi:10.1158/0008-5472.CAN-14-0705.
31. Corbet, C.; Feron, O. Metabolic and mind shifts: from glucose to glutamine and acetate addictions in cancer. *Curr. Opin. Clin. Nutr. Metab. Care* **2015**, *18*, 346–353, doi:10.1097/MCO.0000000000000178.
32. DeBerardinis, R.J.; Mancuso, A.; Daikhin, E.; Nissim, I.; Yudkoff, M.; Wehrli, S.; Thompson, C.B. Beyond aerobic glycolysis: transformed cells can engage in glutamine metabolism that exceeds the requirement for protein and nucleotide synthesis. *Proc. Natl. Acad. Sci. U. S. A.* **2007**, *104*, 19345–19350, doi:10.1073/pnas.0709747104.
33. Hanse, E.A.; Ruan, C.; Kachman, M.; Wang, D.; Lowman, X.H.; Kelekar, A. Cytosolic malate dehydrogenase activity helps support glycolysis in actively proliferating cells and cancer. *Oncogene* **2017**, *36*, 3915–3924, doi:10.1038/onc.2017.36.
34. Kalhan, S.C.; Hanson, R.W. Resurgence of serine: an often neglected but indispensable amino Acid. *J. Biol. Chem.* **2012**, *287*, 19786–19791, doi:10.1074/jbc.R112.357194.
35. Snell, K. Enzymes of serine metabolism in normal, developing and neoplastic rat tissues. *Adv. Enzyme Regul.* **1984**, *22*, 325–400.
36. Possemato, R.; Marks, K.M.; Shaul, Y.D.; Pacold, M.E.; Kim, D.; Birsoy, K.; Sethumadhavan, S.; Woo, H.-K.; Jang, H.G.; Jha, A.K.; et al. Functional genomics reveal that the serine synthesis pathway is essential in breast cancer. *Nature* **2011**, *476*, 346–350, doi:10.1038/nature10350.
37. Locasale, J.W.; Grassian, A.R.; Melman, T.; Lyssiotis, C.A.; Mattaini, K.R.; Bass, A.J.; Heffron, G.; Metallo, C.M.; Muranen, T.; Sharfi, H.; et al. Phosphoglycerate dehydrogenase diverts glycolytic flux and contributes to oncogenesis. *Nat. Genet.* **2011**, *43*, 869–874, doi:10.1038/ng.890.
38. Pollari, S.; Käkönen, S.-M.; Edgren, H.; Wolf, M.; Kohonen, P.; Sara, H.; Guise, T.; Nees, M.; Kallioniemi, O. Enhanced serine production by bone metastatic breast cancer cells stimulates osteoclastogenesis. *Breast Cancer Res. Treat.* **2011**, *125*, 421–430, doi:10.1007/s10549-010-0848-5.
39. Beauvoit, B.; Colombié, S.; Issa, R.; Mazat, J.-P.; Nazaret, C.; Pérès, S. Human-Scale Metabolic Network of Central Carbon Metabolism. Application to serine metabolism from glutamine in Cancer Cells. In *Proceedings of the Évry Spring school on advances in systems and synthetic biology, March 21th-25th, 2016*; Amar, P., Képès, F., Norris, V., Eds.; 2016; pp. 37–56.
40. Kalhan, S.C.; Uppal, S.O.; Moorman, J.L.; Bennett, C.; Gruca, L.L.; Parimi, P.S.; Dasarathy, S.; Serre, D.; Hanson, R.W. Metabolic and genomic response to dietary isocaloric protein restriction in the rat. *J. Biol. Chem.* **2011**, *286*, 5266–5277, doi:10.1074/jbc.M110.185991.
41. Gellerich, F.N.; Gizatullina, Z.; Gainutdinov, T.; Muth, K.; Seppet, E.; Orynbayeva, Z.; Vielhaber, S. The control of brain mitochondrial energization by cytosolic calcium: the mitochondrial gas pedal. *IUBMB Life* **2013**, *65*, 180–190, doi:10.1002/iub.1131.